VIII International Conference on Computational Methods in Marine Engineering
MARINE 2019
R. Bensow and J. Ringsberg (Eds)

NUMERICAL FRICTION LINES FOR CFD BASED FORM FACTOR DETERMINATION

Kadir B. Korkmaz[*†], **Sofia Werner**[†] **and Rickard Bensow**[*]

[*] Department of Mechanics and Maritime Sciences
Chalmers University of Technology
Chalmersplatsen 4, 412 96 Göteborg, Sweden
e-mail: korkmaz@chalmers.se
e-mail: rickard.bensow@chalmers.se

[†] SSPA Sweden AB
Chalmers Tvärgata 10, 412 58 Göteborg, Sweden
email: sofia.werner@sspa.se - Web page: www.sspa.se

Key words: Friction resistance coefficient, form factor, numerical uncertainty, flat plate

Abstract. In this study, frictional resistance coefficients of an infinitely thin 2D plate have been computed at 14 Reynolds numbers (between $log_{10}(Rn) = 6.25$ to 9.5) in sets of five geometrically similar structured grids in order to perform reliable grid dependence studies. Additional grid dependency studies have been performed by using 5 sets of grids which have the same number of cells in all directions but varying first cell sizes normal to the flat plate at $log_{10}(Rn) = 6.25$. Average y^+ values for each grid set for the finest grid varies between 0.0075 and 0.5 (from set 1 to 5 respectively) while none of the simulations exceeded average y^+ value of 1. All simulations were performed with the direct application of the no-slip condition at walls. Therefore, no wall functions were used. Two turbulence models have been used for the investigations: $k-\omega$ SST and EASM. Extensive grid dependence studies have been performed with two different CFD codes SHIPFLOW and FINE™/MARINE, using the same grids. Special attention was paid to the transition from laminar to turbulent flow at the lowest Reynolds number since laminar part can cover a significant part of the plate. At $log_{10}(Rn) = 6.25$ for both CFD codes, laminar flow and transition to turbulent flow was distinctive even though no transition models were applied. Significant dependency on y^+ has been observed with FINE™/MARINE on friction resistance coefficient. On the other hand, SHIPFLOW exhibited less sensitivity to the first cell size variation, hence, revealed smaller numerical uncertainties in general. To ensure a numerical uncertainty of frictional resistance component below 1%, average $y^+ < 0.016$ have been used for generating the data points of friction line with SHIPFLOW for each turbulence model. Data points of 14 Reynolds number have been transformed into numerical friction lines by applying curve fits. Obtained friction lines are compared with ITTC57 line, Schoenherr, Hughes, Toki, Katsui, Grigson lines and two numerical friction lines.

1 INTRODUCTION

The friction line, i.e. the dependency of flat plate frictional resistance coefficients on Reynolds number, is used in the 1978 ITTC method for scaling of ship resistance measured in a towing tank. The 1978 ITTC method adopted the form factor concept as described by Hughes

in [1], where the viscous resistance is expressed in relation to the "ITTC 57 model-ship correlation line" as shown in the following equation:

$$C_V = (1 + k)C_F \tag{1}$$

where k is the form factor and C_F is the friction resistance coefficient. The form factor concept, as well as the determination method proposed by Prohaska [2] has been questioned and investigated for many decades. The scale effects on form factor has been well demonstrated by García-Gómez [3], Toki [4] and Van et al. [5] using geosim test data analysis. In addition to the re-analysis of the geosim test data, CFD studies by Raven et al. [6] and Wang et al. [7] supported the existence of substantial scale effects on form factor and the main cause of the scale effects have been found to be the "ITTC 57 model-ship correlation line" rather than the original hypothesis of Hughes which suggested the form factor is independent of the Reynolds number. Additionally, when the growing disposition to leave the Prohaska's method of form factor determination and growing confidence in numerical resistance calculations are considered, CFD might be able to provide a new method of form factor determination, which can increase the accuracy of the full-scale resistance predictions.

In this study, numerical friction lines have been investigated and two numerical friction lines have been derived with k-ω SST and EASM turbulence models. Grid dependency studies have been performed with SHIPFLOW and FINE™/MARINE codes in order to highlight the aspects that influence the skin friction coefficient, such as the effect of non-dimensional wall distance (y^+), turbulence intensity and transition from laminar to turbulent flow. The study is part of a larger research scope with the goal of recommending suitable procedures for using CFD to derive the form factor and the full scale ship resistance based on towing tank test.

2 FLOW SOLVERS, COMPUTATIONAL DOMAIN, BOUNDARY CONDITIONS AND GRIDS

2.1 Flow Solvers

Two CFD codes have been used for this study: SHIPFLOW 6.3 and FINE™/MARINE 7.2. Starting with the former, XCHAP is the solver of SHIPFLOW which solves the Reynolds averaged Navier-Stokes (RANS) equations with a finite volume method. EASM, as described in [8], and $k-\omega$ SST, of [9], turbulence models are available. The convective terms are discretized with a Roe scheme which is first order accurate. Therefore, in order to increase the accuracy a flux correction is applied explicitly. The equations are solved with Krylov solver (adopted from PETSc) which implements the Generalized Minimal Residual method (KSPGMRES). Note that results from SHIPFLOW will be referred as "SF" in the plots in order to save space.

ISIS-CFD is the flow solver of FINE™/MARINE. The solver is based on Finite volume method and incompressible unsteady Reynolds-averaged Navier Stokes equations are solved. There is no specific requirements on the topology of cells since the face-based method is used. The discretisation of the convective fluxes in both the momentum equations and the equations for turbulence modelling have been performed with AVLSMART scheme for this study. Among many turbulence models available in FINE™/MARINE, EASM, described in [8], and $k-\omega$ SST, of [9], turbulence models have been selected. Note that results from FINE™/MARINE will be referred as "FM" in the plots.

2.2 Computational Domain

The computational domain size is based on the requirements of XCHAP and ISIS-CFD solvers. The domain is shaped as a rectangular prism since a 3D domain is required by the solvers. Size of the domain has been determined by the preliminary computations carried out at $log_{10}(Rn) = 6.25$ with two alternative domains. The flat plate have a length of L. The first domain has the inlet located *0.25L* upstream of the leading edge, the outlet is placed *0.25L* downstream of the trailing edge, side boundary located *0.25L* away from the flat plate in the normal direction. The second domain (Dm2) has been designed with double the distance of the inlet, outlet and side boundaries (*0.5L*). The height of the domain is *1L* for both domains since the flow is 2D and height has no effect on the results.

Table 1 Comparison of influence of domain size on the computed prediction of the friction resistance

	EASM (SHIPFLOW)		EASM (FINE™/MARINE)		$k-\omega$ SST (SHIPFLOW)		$k-\omega$ SST (FINE™/MARINE)	
	g1	g5	g1	g5	g1	g5	g1	g5
$\Delta C_F(\%)$	-0.6	-0.6	-0.6	-0.7	-0.6	-0.6	-0.6	-0.6
$U(C_F)(\%)$								
Dm1	0.08	0.29	0.13	0.37	0.18	0.69	0.09	0.32
Dm2	0.08	0.28	0.10	0.36	0.17	0.63	0.10	0.35

The differences between the frictional resistance coefficients for the two domain sizes, $\Delta C_F(\%) = 100 \times (C_F(Dm2) - C_F(Dm1))/C_F(D1)$, together with obtained numerical uncertainties, $U(C_F)$, for the finest grid are presented in Table 1. The differences in C_F between the two domains are larger than the numerical uncertainties (presented in Section 3), opposed to what was observed by Eça and Hoekstra [10]. The investigations have indicated that the difference might originate from the dissipated turbulent kinetic energy between the inlet boundary and the flat plate. As it will be more thoroughly discussed in the Section 2.4, larger domain (Dm2) seems to act as a flow with lower turbulence intensity which results in slightly delayed transition from laminar to turbulent flow and lower friction resistance in the turbulent region. In order to confirm this argument, additional simulations have been performed with Dm2 domain at $log_{10}(Rn) = 8.00$. The difference of C_F has been reduced to the numerical uncertainty levels as at such high Reynolds numbers turbulence intensity is not expected to have substantial impact. In the light of these findings the initial domain, Dm1, has been chosen for the further computations.

2.3 Boundary Conditions

The inlet boundary conditions are fixed uniform velocity (U_∞) and specific turbulent dissipation rate, ω, at the inlet is calculated by $(\omega)_{inlet} = \lambda U_\infty / L$. The default values of the factor of proportionality, λ, are set to $\lambda = 1$ for FINE™/MARINE and $\lambda = 10$ for SHIPFLOW. The turbulent kinetic energy at the inlet is defined as $(k)_{inlet} = \mu \omega_{inlet} C_i / \rho$ where μ and ρ are dynamic viscosity and density respectively. FINE™/MARINE assumes the value of the constant $C_i = 1 \times 10^{-3}$ while SHIPFLOW adopted $C_i = 1 \times 10^{-4}$. As a result, both codes have the same turbulence intensity at the inlet. The outlet boundary condition of both codes consists of Neumann boundary condition that sets the gradient of velocity, k and pressure to zero,

normal to the outflow plane. Slip condition simulates a symmetry condition by setting the normal velocity and normal gradient of other variables to zero. Noslip condition specifies the velocities components, k and normal pressure component as zero at the wall. ω on the wall is specified differently by both codes. For FINE™/MARINE, $\omega_w = 10 \times (6\mu/0.075\rho d^2)$ where d is the distance of the first cell away from the wall. SHIPFLOW defines the wall value of ω of a smooth surface as $\omega_w = (u_\tau^2/\nu) \times \left(50/4.3y^{+0.85}\right)^2$ as introduced in [11] where $u_\tau$is he frictional resistance and ν is the kinematic viscosity. All simulations have been performed with the direct application of the no-slip condition at walls. Therefore, no wall functions were used.

2.4 Local skin friction coefficient and transition from laminar to turbulent flow

Local skin friction coefficients of have been investigated in order to assess the behaviour of turbulence models in transition from laminar to turbulent flow. The local skin friction coefficient has been defined as:

$$C_f = \frac{\mu\left(\frac{\partial u_x}{\partial y}\right)_{y=0}}{\frac{1}{2}\rho U_\infty L} \tag{2}$$

At the typical Rn that towing tank model tests are normally performed, transition is considered to be important. As indicated by Eça et al. [10], the natural transition in the boundary layer of a flat plate occurs approximately at $Re_x = 10^6$. However, the transition can occur earlier if the turbulence intensity is increased. In this study, no transition models have been used as the aim is to determine the behaviour of the regular turbulence models readily available in both SHIPFLOW and FINE™/MARINE.

The calculated skin friction coefficients from SHIPFLOW and FINE™/MARINE at $log_{10}(Rn) = 6.25$ are presented in Figure 1 together with the ERCOFTAC Classic Database [12] where flat plate experiments with three different free-stream turbulence intensity ($0.009U_\infty^2$, $0.03U_\infty^2$ and $0.06U_\infty^2$) were performed. The turbulence intensity at the inlet boundary with SHIPFLOW and FINE™/MARINE are the same, $k_\infty \cong 5.6 \times 10^{-10} U_\infty^2$ for $log_{10}(Rn) = 6.25$. The first significant observation is the laminar flow region where C_f of both turbulence models and CFD codes follow Blasius line until the transition to turbulent flow occurs. If laminar flow covers a significant part of the plate, the calculated skin friction coefficient will be smaller than a fully turbulent flow. However, both turbulence models and CFD solvers predicted the transition location approximately where the turbulence stimulators are usually fitted to towing tank ship models (5% of L_{pp} from fore perpendicular). The position of the transition is similar to ERCOFTAC experiments with 3% and 6% even though turbulence intensity in the computations are extremely smaller than the experiments. It is also significant that the transition shows qualitatively similar behaviour to the experiments with both $k-\omega$ SST and EASM turbulence models with both solvers. The laminar flow can be observed even at Rn numbers as high as $log_{10}(Rn) = 9.5$ as presented in Figure 1 even though only a fraction of the flat plate (~0.003%) is covered with laminar flow. As can be seen from the Figure 1 (on the right), simulations at different Reynolds numbers show consistency in skin friction coefficient not only at the laminar region but also at the turbulent region. It should be noted that, the vertical lines occurs due to local increase of C_f at the trailing edge of the flat plate.

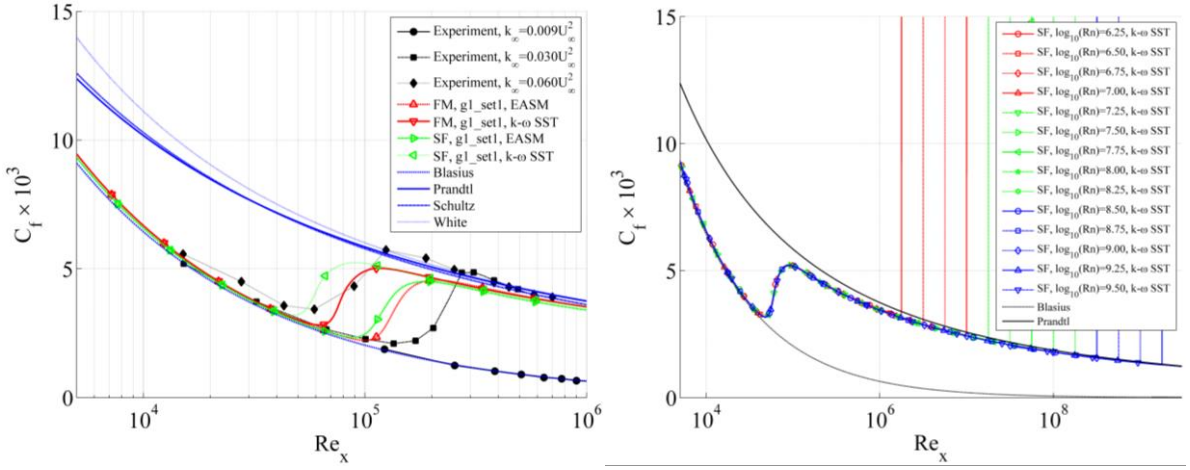

Figure 1 Skin friction coefficient C_f along the flat plate at $log_{10}(Rn) = 6.25$ (on the left) and C_f along the flat plate at $log_{10}(Rn) = 6.25$ to 9.5

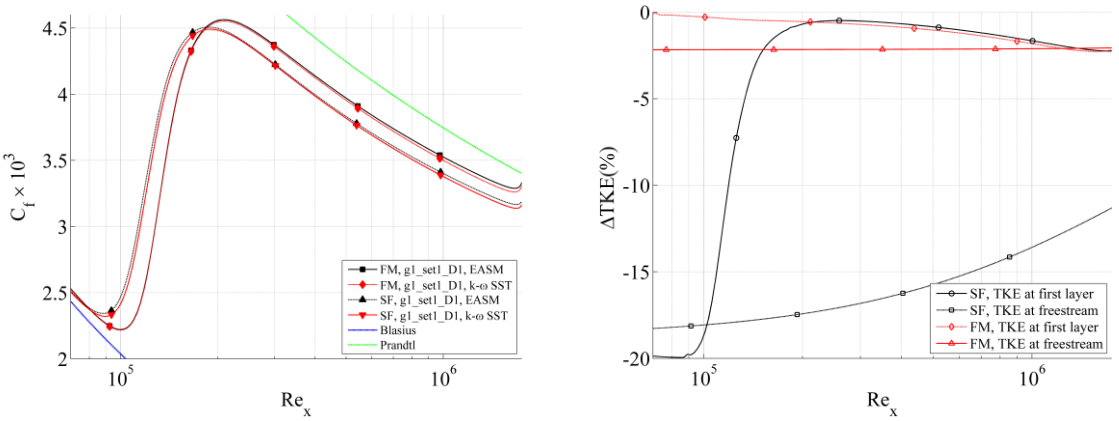

Figure 2 Influence of domain size on TKE and on the skin friction coefficient along the flat plate at $log_{10}(Rn) = 6.25$. $\Delta TKE(\%) = 100 \times (TKE(Dm2) - TKE(Dm1))/TKE(D1)$

As mentioned previously, the increase of the domain size resulted in a reduction of C_F approximately 0.6% which is significantly larger than the numerical error for both codes. The investigations have shown that with a larger domain size (Dm2), the turbulent kinetic energy (TKE) dissipates more than with the smaller domain (Dm1). The difference of TKE between the domains has been calculated as $\Delta TKE(\%) = 100 \times (TKE(Dm2) - TKE(Dm1))/TKE(Dm1)$. As shown in Figure 2 (on the right), the freestream TKE levels are approximately -18.8% and -2.1% lower in Dm2 compared to Dm1 domain at the alignment in x-direction of the leading edge of the plate for SHIPFLOW and FINE™/MARINE respectively. The reason of such difference in TKE dissipation levels is explained by the different boundary condition of $(\omega)_{inlet}$ which is ten times larger in SHIPFLOW than FINE™/MARINE. TKE at the first layer away from the plate with Dm2 are also lower than Dm1 all over the Re_x range. As shown in Figure 2, the transition has been slightly delayed in SHIPFLOW simulation and the C_f values are lower with an increasing rate from the transition location (where TKE levels are similar in both domains around $Re_x = 2 \times 10^5$) to the trailing edge where C_f is approximately 0.8% lower in Dm2 than Dm1 case for both codes. This means that the domain size has an effect on the TKE that gives a non-negligible impact on the total skin friction.

2.5 Grid Sets

The discretization of the computational domain has been done by five sets (sets 1 to 5) of orthogonal stretched grids. Each set consists of five geometrically similar grids. Grid sets have the same number of cells along the x-direction and y-direction but differing in the first cell size perpendicular to the flat plate for the corresponding Reynolds number. The smallest first cell sizes in y-direction (yielding lowest y^+ values) are denoted as set1 and first cell sizes are gradually increased from set1 to set5 having the largest y^+ values. In all the grids, the number of cells along the plate makes *4/6* of all the cells in x-direction, leaving 1/6 of cells for upstream and downstream of the plate. The cells in the normal direction has been stretched with a one sided stretching function. The leading edge and trailing edges are also stretched in a similar fashion. The five geometrically similar grids of each set have been refined with grid refinement ratio of $h_i/h_1 = \sqrt{N_{cells_1}/N_{cells_i}}$. The number of cells corresponding to each grid and flow speed are presented in Table 2. In order to assure growth rate of the cells in y-direction (normal to the plate) remain in similar levels throughout the Rn range, three different mesh density have been used.

Table 2 Number of cells in each direction

	g1		g2		g3		g4		g5	
lo10Rn	Nx	Ny	Nx	Ny	Nx	Ny	Nx	Ny	Nx	Ny
6.25-7.0	1440	240	1260	210	1080	180	900	150	720	120
7.25-8.25	2160	360	1890	315	1620	270	1350	225	1080	180
8.5-9.5	2880	480	2520	420	2160	360	1800	300	1440	240

Table 3 Calculated $(y^+)_{mean}$ and $(y^+)_{max}$ values from SHIPFLOW at the first layer away from the flat plate for EASM turbulence model at $log_{10}(Rn) = 6.25$

	$(y^+)_{mean}$					$(y^+)_{max}$				
	set1	set2	set3	set4	set5	set1	set2	set3	set4	set5
g1	0.008	0.057	0.105	0.238	0.448	0.09	0.53	0.90	1.73	2.66
g2	0.009	0.065	0.120	0.272	0.512	0.10	0.59	1.00	1.88	2.88
g3	0.010	0.076	0.140	0.318	0.598	0.11	0.66	1.12	2.08	3.15
g4	0.012	0.091	0.167	0.381	0.719	0.13	0.76	1.27	2.33	3.50
g5	0.016	0.113	0.209	0.477	0.900	0.15	0.90	1.48	2.66	3.96

The first layer cell size is varied with the same ratio (h_i/h_1) for each grid set. In Table 3, mean and maximum y^+values for computations from SHIPFLOW at $log_{10}(Rn) = 6.25$ have been presented. The y^+ values from FINE™/MARINE were almost identical to Table 3. All simulations have been performed with $(y^+)_{mean} < 1$ which is the widespread rule of thumb. The $(y^+)_{max}$ values exceeds the non-dimensional height of $y^+ = 1$ for set3 to set5, however, it is observed only at the very ends of leading and trailing edges of the plate. For a given Reynolds number (the speeds other than $log_{10}(Rn) = 6.25$), first cells sizes has been adjusted so that similar $(y^+)_{mean}$ values are obtained as presented in Table 3.

It is important to note that SHIPFLOW solver does not have 2D flow option therefore 3 cells are added in the z-direction which is the only way they differ from the meshes used for FINE™/MARINE. To ensure FINE™/MARINE solver provides the same results for 2D and

3D meshes, several computations have been performed and no significant difference has been found. Therefore, 2D grids have been calculated with ISIS-CFD solver in order to save time and reduce the computational demand.

3 GRID DEPENDENCE STUDY

In order to assess the numerical uncertainty, grid dependence studies have been performed. All computations have been performed in double precision in order to eliminate the round-off errors. Additionally, iterative uncertainties have been predicted from the standard deviation of the force in percent of the average force over the last 10% iterations. Iterative uncertainty was kept below 0.01% for all simulations. Simulations at $log_{10}(Rn) < 8$ exhibited even lower standard deviations of force (typically lower than 1×10^{-4}). Therefore, both iterative errors and round-off errors are assumed to be small enough to be neglected and numerical errors are dominated by the discretization errors. The procedure proposed in [13] have been adopted to predict the numerical uncertainties.

Table 4 Observed order of accuracy, p, for the flat plate at $log_{10}(Rn) = 6.25$

	SHIPFLOW					FINE™/MARINE				
	set1	set2	set3	set4	set5	set1	set2	set3	set4	set5
EASM	1.9	1.9	1.6	1.1	1.5	1.5	1.4	1.2	0.9	0.6
$k-\omega$ SST	2	2	1.8	1.1	0.9	1.8	1.4	1.1	0.8	0.5

Table 5 Predicted numerical uncertainties, $U(C_F)$, for EASM turbulence model, in percentage

	SHIPFLOW						FINE™/MARINE				
	set1	set2	set3	set4	set5		set1	set2	set3	set4	set5
g1	0.08	0.10	0.18	0.55	0.62	g1	0.13	0.41	0.86	2.48	6.15
g2	0.10	0.13	0.22	0.64	0.76	g2	0.16	0.50	1.01	2.79	6.65
g3	0.14	0.17	0.29	0.76	0.94	g3	0.20	0.62	1.21	3.19	7.28
g4	0.19	0.24	0.39	0.93	1.24	g4	0.26	0.79	1.50	3.74	8.12
g5	0.29	0.36	0.55	1.19	1.71	g5	0.37	1.08	1.95	4.55	9.26

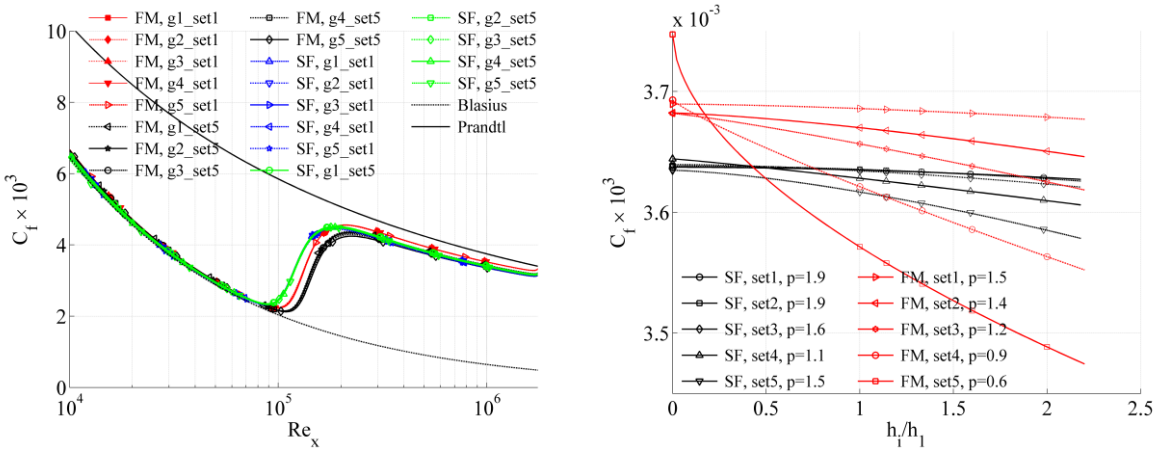

Figure 3 Influence of first cell size (set1 and set5) on the skin friction coefficient along the flat plate and convergence of friction coefficient C_F for SHIPFLOW and FINE™/MARINE at $log_{10}(Rn) = 6.25$

The observed order of accuracies and numerical uncertainties for SHIPFLOW and FINE™/MARINE are presented in Table 4 and Table 5. The numerical uncertainties from *k-ω* SST model is slightly higher than EASM for all grid sets with FINE™/MARINE. However, predicted uncertainties on set 1 and set2 with k-*ω* SST are almost two times higher with SHIPFLOW. The ISIS-CFD solver have been found to be sensitive to near wall cell height compared to XCHAP solver since numerical uncertainties on the skin friction coefficient can be as high as 9% with $(y^+)_{mean}$ values around 0.9.

In order to explain the difference of $U(C_F)$ between the two solvers, the skin friction coefficient along the flat plate has been investigated. As presented in Figure 3, the grids belong to set1 and set5 has been plotted for SHIPFLOW and FINE™/MARINE. It is important to notice that C_f values from SHIPFLOW are consistent in set1 and set5 grids in the laminar region and transition location but differing marginally in the turbulent region. However, for FINE™/MARINE the C_f values are consistent in the laminar region but differing significantly between set1 and set 5 for the transition location also in the fully turbulent region (up to 5% difference in C_f). Sensitivity to y^+ can also be observed with convergence of C_f with the grid refinement presented for EASM model for both solvers in Figure 3. It is worth to recall that the number of cells corresponding to each h_i/h_1 value ($h_i/h_1 = 1$ being the finest grid) are identical. Considering the numerical uncertainties presented, it can be concluded that $(y^+)_{mean} \cong 1$ is not acceptable for any of the solvers and in order to attain $U(C_F)$lower than 1%, $y^+ \cong 0.1$ should be used for *k-ω* SST and EASM turbulence models, as also concluded by Eça et all. [14].

Considering the outcomes of the grid dependence study performed at $log_{10}(Rn) = 6.25$, the rest of the simulations have been performed with 5 geometrically similar grids per speed with y^+ values similar to the set1 presented in Table 3 .Observed order of accuracies and predicted numerical uncertainties for the finest grids are presented in Table 6 and Table 7.

Table 6 Observed order of accuracy,p, of the friction resistance for SHIPFLOW

	$\log_{10}(Rn)$													
	6.25	6.5	6.75	7	7.25	7.5	7.75	8	8.25	8.5	8.75	9	9.25	9.5
EASM	1.9	1.8	1.7	1.7	1.8	1.9	1.8	1.7	1.7	2	1.8	1.7		
$k-\omega$ SST	2	2	2	2	2	2	1.2	2	2	2	2	2	2	2

Table 7 Predicted numerical uncertainties of the finest girds (g1), of the friction resistance, $U(C_F)$, for SHIPFLOW, in percentage

	$\log_{10}(Rn)$													
	6.25	6.5	6.75	7	7.25	7.5	7.75	8	8.25	8.5	8.75	9	9.25	9.5
EASM	0.08	0.10	0.12	0.13	0.06	0.06	0.07	0.09	0.08	0.04	0.05	0.05		
$k-\omega$ SST	0.18	0.21	0.25	0.29	0.10	0.11	0.14	0.14	0.15	0.04	0.09	0.08	0.08	0.05

4 NUMERICAL FRICTION LINE

The friction resistance coefficient C_F is obtained from the integration of the C_f along the flat plate. As explained earlier, C_F of 5 geometrically similar grids for 14 Reynolds number has been calculated with $k-\omega$ SST and EASM turbulence models with SHIPFLOW. The last two

speeds with EASM are omitted due to difficulties with convergence issues. As a result of performing the grid dependence study as explained by Eça and Hoekstra [13], the exact numerical solution of friction resistance coefficient at each Reynolds number have been calculated. The exact solutions or in other words grid independent results, are then used for the generation of numerical friction lines. Curve fits have been applied to data generated using the two alternative formulations. The first alternative is based on the ITTC 57 analytical formula

$$C_F^a = \frac{a_1^a}{(\log_{10}(Rn) - a_2^a)^{a_3^a}} \tag{3}$$

The second alternative as adopted from [10] assumes that C_F can be expressed as a cubic polynomial in logarithmic scales

$$\log(C_F^c) = \log(a_1^c) + a_2^c \log(Rn) + a_3^c (\log Rn)^2 + a_4^c (\log Rn)^3 \tag{4}$$

Eq. 4 can be re-formulated as the following

$$C_F^c = a_1^c (Rn)^{(a_2^c + a_3^c \log(Rn) + a_4^c (\log Rn)^2)} \tag{5}$$

The three constants a_1^a, a_2^a and a_3^a of Eq. 3 and the four constants a_1^c, a_2^c, a_3^c and a_4^c of Eq. 5 have been determined with a non-linear least squares approach. In order to assess the quality of the fit, root-mean-square error (denoted as S) has been calculated by determining the degree of freedom by the difference between the number of data points and number of constraints. The constants and the standard deviations of the two equations have been presented in Table 8.

Table 8 Constants of the curve fits for of Eq. 3 and Eq. 5 to the friction coefficients of EASM and k-ω STT turbulence models

	C_F^a				C_F^c				
	a_1^a	a_2^a	a_3^a	$S^a \times 10^6$	$a_1^c \times 10^2$	$a_2^c \times 10^2$	$a_3^c \times 10^3$	$a_4^c \times 10^5$	$S^c \times 10^6$
EASM	11.300	-3.617	3.512	5.329	1.792	-2.400	-9.40	23.40	2.796
$k-\omega$ SST	0.612	-0.592	2.638	2.383	10.810	-30.75	5.81	-3.96	1.627

The curve fits of Eq.3 and Eq.5 shows both very good agreement with the data. The differences between the two fits are graphically hard to assess since they are almost coinciding throughout the Rn range. However, the root-mean-square error indicates that Eq.5 is the better fit for both turbulence models. Therefore, Eq. 5 is adopted and compared to the other friction lines. Obtained numerical frictional lines for *k- ω* SST and EASM turbulence models have been compared with ITTC57 line [15], Schoenherr [16], Hughes [1], Toki [4], Katsui [17], Grigson [18] and two numerical friction lines proposed by Eça et al. [10] and Wang et al. [7]. Figure 4 presents the friction lines in a relative way because the visual judgement over the friction lines is difficult when presented many lines at a time. The differences between the friction lines are presented with respect to numerical friction derived from *k- ω* SST model of SHIPFLOW and calculated, i.e. $\Delta C_F(ITTC57)\ (\%) = 100 \times (C_F(ITTC57) - C_F(\mathrm{k}-w\ SST))/C_F(\mathrm{k}-w\ SST)$. As can be seen from Figure 4, *k-ω* SST lines of Eça et al. [10] and Wang et al. [7] are very similar to *k-ω* SST line derived by SHIPFLOW in all Reynolds numbers. The spread among the numerical friction lines is much smaller than analytical friction lines in general. All numerical friction lines lead to lower C_F values than the analytical correlations (except Hughes line) at the lower Rn range but the gap is reduced around $log_{10}(Rn) = 8.0$ and onwards. Existence of

laminar flow in the lowest Reynolds numbers for the numerical friction lines can be responsible for such behavior which should be investigated further.

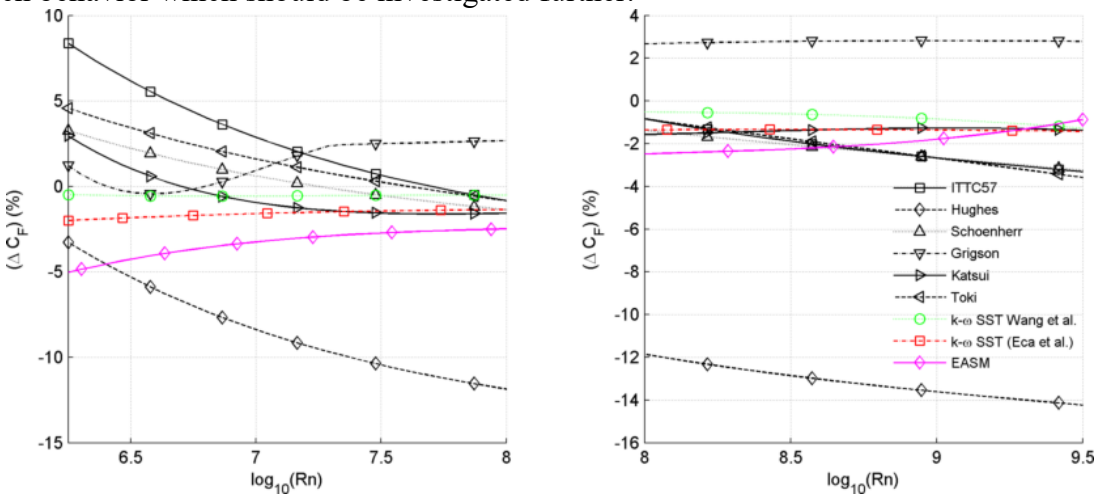

Figure 4 Friction lines in comparison to SHIPFLOW $k-\omega$ SST, in percentage

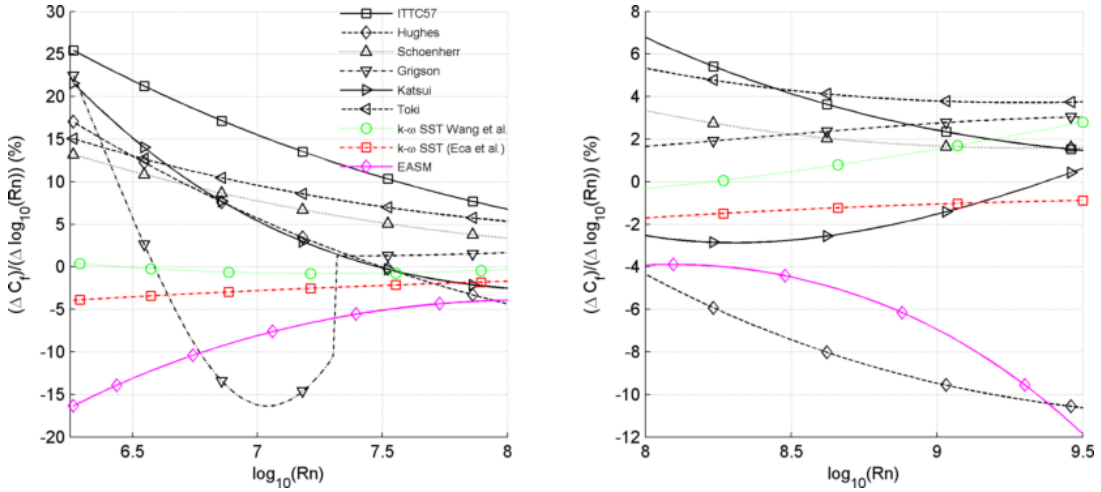

Figure 5 Derivative of the friction lines in comparison to SHIPFLOW $k-\omega$ SST, in percentage

The slope of the friction line is more important than the absolute values for the purpose of extrapolation. Therefore, the derivatives of the lines have been calculated and presented in Figure 5, again with respect to k-ω SST line of SHIPFLOW. The similarity of k-ω SST lines of Eça and Hoekstra [10] and Wang et al. [7] to the k-ω SST line derived from SHIPFLOW is remarkable. All numerical friction lines possess significantly lower slope at the lower range of Reynolds numbers, but this difference is reduced significantly at $Rn < 10^8$ except Hughes lines and the friction line derived from EASM turbulence model. The slope obtained with EASM is distinctively smaller at the both ends of the Reynolds numbers.

5 CONLUSIONS

This paper presents a study on the numerically calculated friction resistance coefficient of an infinitely-thin flat plate as a function Reynolds number in the range of $6.25 < log_{10}(Rn) < 9.5$. EASM and k-ω SST turbulence models have been used and investigated. Comprehensive

grid dependence studies have been performed with SHIPFLOW and FINE™/MARINE codes. Two numerical friction lines are derived from the SHIPFLOW and compared to the lines available in open literature.

The grid dependence studies at $log_{10}(Rn) = 6.25$ indicated that numerical uncertainty on the friction resistance coefficient is highly dependent on the first cell size. In order to achieve numerical uncertainty of frictional resistance coefficients below 1%, SHIPFLOW requires approximately $y^+ \leq 0.4$ for both EASM and k-ω SST models. However, the requirement to achieve numerical uncertainties below 1% for FINE™/MARINE is $y^+ \leq 0.1$ for both EASM and k-ω SST models which was also the conclusion of [14] for the latter turbulence model.

Two main modelling errors have been investigated: transition of flow from laminar to turbulent and turbulence models. Laminar to turbulent transition has been observed in both turbulence models and CFD solvers. Even though, transition location was predicted differently by the two CFD codes, transition behavior was qualitatively correct compared to ERCOFTAC experiments. Comparing the turbulence intensity levels at ERCOFTAC experiments to the very low turbulence intensity levels in CFD, transition occurs at too low Reynolds numbers with CFD. When the location of the transition is analyzed, only around 5% of the plate featuring the laminar flow at the lowest Rn. Considering that the turbulence stimulators in model testing are usually placed at 5% of L_{pp} from the fore perpendicular, amount of wetted surface covered by laminar flow in a model test is comparable to the numerical conditions.

The numerical calculations with two different domain sizes indicated that the effect of turbulence intensity at the leading edge affects the calculated friction resistance. Obviously, the slope of the friction line at the lower Reynolds number will change depending on which turbulence intensity have been chosen. Its implications are not investigated within the context of this study.

Numerical friction lines have been obtained for EASM and k-ω SST turbulence models using SHIPFLOW. The expression based on cubic polynomial in the logarithmic scales (Eq.5) provided the best fit for both turbulence models. The derived numerical friction lines were compared to the friction lines available in open literature. The slope of the line derived from k-ω SST is similar to other the numerical friction lines of Eça and Hoekstra [10] and Wang et al. [7] of the same turbulence model. EASM line exhibits significantly less slope at the both ends of the Rn range and differing from all other friction lines in the high Rn range except the Hughes line to some extent.

When using a numerical friction line for ship resistance extrapolation it should be considered that the result could be highly dependent on several factors: non-dimensional wall distance (y^+), choice of turbulence model, boundary conditions such as turbulence intensity and the CFD code. Since numerical approaches differ for each code, the effect of these factors can be different as well. Hence, it may not be advisable to use a general friction line for CFD based form factor determination method. The next step in our research is to study the previously mentioned factors that may affect the ship resistance extrapolation.

REFERENCES

[1] G. Hughes, “Friction and Form Resistance in Turbulent Flow, and a Proposed Formulation for Use in Model and Ship Correlation”. *Trans. RINA*, Vol. 96, (1954) p.314-376

[2] C. W. Prohaska, “A Simple Method for the Evaluation of the Form Factor and Low Speed

Wave Resistance", *Proceeding of 11th ITTC*, (1966).

[3] A. García-Gómez, "On the Form Factor Scale Effect", *Ocean Engineering*, Vol 26, (2000) pp.97-109.

[4] N. Toki, "Investigation on Correlation Lines through the Analyses of Geosim Model Test Results", *Journal of the Japan Society of Naval Architects and Ocean Engineers*, Vol 8, (2008). pp.71-79

[5] S.-H.Van, H. Ahn, Y.-Y. Lee, C. Kim, Hwang, S. Hwang, J. Kim, K.-S. Kim, I.-R. Park, "Resistance Characteristics and Form Factor Evaluation for Geosim Models of KVLCC2 and KCS", *Advanced Model Measurement Technology for EU Maritime Industry*, (2011) pp.282-293.

[6] H. C. Raven, A. van der Ploeg, A.R. Starke, L. Eça, "Towards a CFD-based prediction of ship performance --- progress in predicting full-scale resistance and scale effects", *International Journal of Maritime Engineering*, Vol. 135, (2009).

[7] Z.-z. Wang, Y. Xiong, L.-p. Shi, Z,-h, Liu, "A Numerical Flat Plate Friction Line and Its Application", *Journal of Hydrodynamics*, Vol 23 (3), (2015) pp.383-393.

[8] G. B. Deng and M. Visonneau, "Evaluation of eddy- viscosity and second- moment turbulence closures for steady flows around ships,", *21st ONR Symposium on Naval Hydrodynamics*, (1996) pp. 453–469.

[9] F. Menter, "Two-equation Eddy-viscosity turbulence models for engineering applications", *AIAA Journal* Vol.32 no. 8 (1994) pp.1598-1605

[10] L. Eça and M. Hoekstra, "The numerical friction line", *Journal of Marine Science and Technology*, Vol 13, (2008) pp. 328-345.

[11] A. Hellsten Some improvements in Menter's k-omega SST turbulence model, *29th AIAA, Fluid Dynamics Conference*, Fluid Dynamics and Co-located Conferences, (1998)

[12] ECOFTAC Classic Collection Database -http://cfd.mace.manchester.ac.uk/ercoftac

[13] L. Eça and M. Hoekstra, "A Procedure for the Estimation of the Numerical Uncertainty of CFD Calculations Based on Grid Refinement Studies", *Journal of Computational Physics*, Vol 262, (2014) pp. 104-130.

[14] L. Eça, F.S. Pereira, G. Vaz, "Viscous flow simulations at high Reynolds numbers without wall functions: Is y+ ≅ 1 enough for the near-wall cells?", *Computers and Fluids,* Vol. 170, (2018) pp.157-175

[15] Proceedings of the 8th ITTC, Madrid, 1957

[16] Karl E. Schoenherr, "Resistance of flat plate surfaces", *Trans. SNAME* (1932) 40:279-313

[17] T. Katsui, H. Asai, Y. Himeno, Y. Tahara, "The Proposal of a New Friction Line" *Fifth Osaka Colloquium on Advanced CFD Applications to Ship Flow and Hull Form Design*, Osaka, Japan, (2005).

[18] C.W.B. Grigson, "A planar algorithm and its use in analysing hull resistance". *Trans. RINA*, Vol 142, (1999) pp. 76-115.